Inorganic Chemistry

Article

pubs.acs.org/IC

Staple Motifs, Initial Steps in the Formation of Thiolate-Protected Gold Nanoparticles: How Do They Form?

Víctor Rojas-Cervellera,[†,‡,∥] Ernest Giralt,[⊥,∥] and Carme Rovira*[,†,‡,¶,∥]

[†]Computer Simulation and Modeling Laboratory, Parc Científic de Barcelona, Baldiri Reixac 10−12, 08028 Barcelona, Spain

[‡]Institut de Química Teòrica i Computacional, Diagonal 647, 08028 Barcelona, Spain

[⊥]Institut de Recerca Biomèdica de Barcelona, Parc Científic de Barcelona, Baldiri Reixac 10−12, 08028 Barcelona, Spain

[∥]Departament de Química Orgànica, Universitat de Barcelona, Diagonal 647, 08028 Barcelona, Spain

[¶]Institució Catalana de Recerca i Estudis Avançats, Passeig Lluís Companys 23, 08018 Barcelona, Spain

Supporting Information

ABSTRACT: Recent structural determinations have shown that thiolate-protected gold nanoparticles are not as regular and symmetric as initially thought, but characteristic substructures (*staple motifs*) are formed on their surface. However, their mechanism of formation, especially the fate of the sulfur protons upon thiol binding, remains one of the most intriguing unanswered questions in gold cluster chemistry. By means of ab initio molecular dynamics (AIMD), we monitor the *trajectory* of thiol protons reacting with a gold cluster, demonstrating that the staple motif forms in a multiple-pathway chemical reaction, releasing molecular hydrogen. The results obtained also reconcile the conclusions of structural determinations with the interpretations of spectroscopic experiments on solution, suggesting the presence of intact thiols or chemisorbed hydrogen.

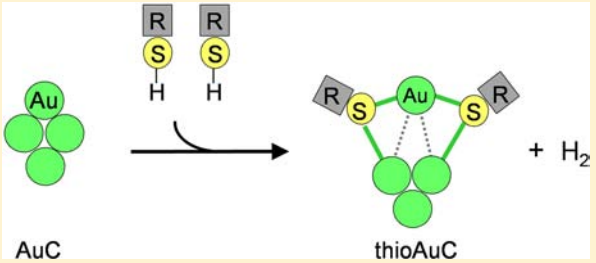

1. INTRODUCTION

Gold clusters and nanoparticles (AuCs and AuNPs) have excited much interest not only because of their electronic properties[1] but also because of their broad range of technological applications, such as molecular electronics,[2] catalysis, and biosensors.[3] In biomedicine, AuNPs are used as antiarthritic and antitumor drugs.[4] The observation that small enough nanoparticles (around 10 nm) cross cell membranes and can be used as peptide transporters[5] opens the door for a number of therapeutic applications, such as the treatment of Alzheimer's disease.[6] Key to these experiments is the capacity to *decorate* the nanoparticles with thiols (e.g., peptides that bind through the sulfur atom of a terminal cysteine residue).[7]

Although the classical synthetic strategy of thiolate-protected AuNPs consists of the reduction of a preformed $Au^{I}SR$ polymer (R = organic group), experiments on lipoate-coated nanoparticles[8] have demonstrated that the thiolate layer can also form from a neutral AuNP. In addition, recent analyses using the solvated metal atom dispersion method provide evidence of hydrogen evolution upon exposure of thiols to AuCs,[9] due to S−H bond scission. These experiments indicate that a redox reaction occurs between the neutral gold atoms and the protons of the incoming thiols. Not surprisingly, protons have been proposed as oxidants for gold(0).[10]

From a structural point of view, several studies[11] have shown that the gold atoms of AuCs and AuNPs do not form a compact gold core, but some gold atoms emerge from the surface, interacting strongly with the sulfur atoms (Figure 1). The latter surround the inner gold core and form characteristic substructures, named *staple motifs*,[11a] as was first reported for self-assembled monolayers (SAMs) on a gold surface.[12] Interestingly, a recent theoretical study shows that the staple motif is the preferred structural unit for a medium-sized AuC.[13] The presence of conserved staple substructures in all AuCs/AuNPs so far characterized suggests that there is a general mechanism by which these substructures form. Key to deciphering this mechanism is to rationalize how the simplest thiolate−gold substructure, the monomeric staple, is formed from its neutral thiol and AuC precursors.

Notwithstanding the amount of experimental and theoretical studies on AuCs and AuNPs (see, for instance, refs 10, 11, 13 and 15−17), the molecular mechanism of the chemical reaction leading to the formation of Au−S bonds, such as the ones that constitute the staple motifs, remains a mystery. Specifically, the fate of the protons released during thiol binding,[16] from its neutral unbound form (RSH) to the anionic bound form (SR), and the atomic/electronic rearrangements upon formation of staple motifs[11a] remain controversial issues. Only thiolate−gold bonds, in the form of staple motifs, are found in X-ray structures of monolayer-protected AuCs. However, a signal of hydrogen atoms was detected in NMR spectroscopic measurements,[16] suggesting the presence of intact thiols on their surface, without excluding the fact that hydrogen could be adsorbed on the gold

Received: May 23, 2012
Published: October 10, 2012

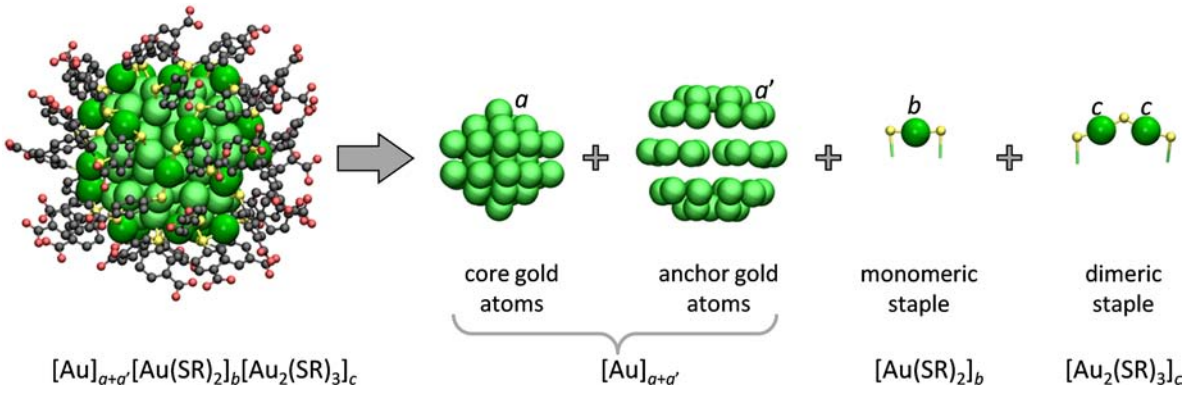

Figure 1. Molecular structure of $Au_{102}(p\text{-MBA})_{44}$ (p-MBA = p-mercaptobenzoic acid) and its building blocks according to the elegant "divide-and-protect" scheme.[14] Organic groups attached to the sulfur atoms (R) in the right part of the figure are not shown for clarity. Sulfur atoms are in yellow and gold atoms in green. Types of gold atoms: gold atoms bound "only" to other gold atoms (type a); gold atoms bound "only" to thiolates (types b and c); gold atoms bound to both gold atoms and thiolates (type a′). $[Au]_{a+a'}$ represents the inner gold core, whereas $[Au(SR)_2]_b$ and $[Au_2(SR)_3]_c$ are the monomeric and dimeric staples,[11a,c,14,15] respectively. From the point of view of a formal oxidation state, each thiolate withdraws one electron from the system. Note that a and a′ are used either to refer to the type of gold atom or the number of gold atoms of a given type. The pictures have been drawn with VMD.

surface (i.e., H−Au bonds). Therefore, a current lack of mechanistic insight does not allow firm conclusions regarding the molecular details of the mechanism.

We report an ab initio metadynamics study showing that a gold−thiol complex readily evolves in a multiple-pathway chemical reaction to form a *monomeric staple motif*, as is present on the surface of thiolate-protected AuCs. A number of intermediate species, including those proposed in experimental studies, are found during the chemical redox reaction. We also present theoretical evidence for the release of molecular hydrogen upon the formation of Au−S bonds in a thioAuC. The results obtained reconcile the findings of previous spectroscopic techniques (intact thiols or chemisorbed hydrogen) with those obtained by X-ray measurements (thiolate−sulfur bonds). Finally, a general mechanism to explain the protection of AuCs by thiol groups is proposed. While this paper was being revised, a density functional theory (DFT) study of methylthiol interaction with models of a Au(111) surface was published.[18] Although the techniques used are quite different (geometry optimizations in the study of Askerka et al.[18] and ab initio metadynamics in our work), both studies provide evidence of the release of molecular hydrogen upon the formation of one staple motif.

2. COMPUTATIONAL DETAILS

2.1. Models. To elucidate the molecular mechanism of the redox reaction, we designed the smallest thioAuC bearing one monomeric staple motif. This model system must conform to the stoichiometric relations governing the size of thiolate-protected AuCs [see the Supporting Information (SI), pp S2 and S3]. The $Au_4(SR)_2$ cluster, which can also be expressed as $[Au]_{1+2}[Au(SR)_2]_1$ fulfills these requirements. It contains one gold core atom ($a = 1$), two gold anchor atoms ($a' = 2$), and one monomeric staple motif ($b = 1$ and $c = 0$; Figure 1). Moreover, the number of valence electrons (2) is the smallest possible "magic number" (see the SI, p S2, eq 4).[19]

Other thiolate-protected AuCs with two valence electrons have been proposed by Jiang et al.,[20] such as $Au_{10}(SR)_8$, $Au_8(SR)_6$, $Au_6(SR)_4$, or $Au_{12}(SR)_9^+$. However, we rely on $Au_4(SR)_2$ because of its smaller size. Monomeric staples have been characterized in the solid state for an Au_4 cluster[21] and, therefore, they should be stable.

For the sake of simplicity, the thiol groups will be taken as methylthiols (CH_3SH). The stability of the $Au_4(SR)_2$ system was initially tested by ab initio molecular dynamics (AIMD) at room temperature (see the SI, pp S3 and S4). The $Au_4(SR)_2$ cluster was found to be stable under optimization and further molecular dynamics simulation, with structural parameters in good agreement with the data available for larger clusters.[11a,c,15]

Given the above considerations, the question of the mechanism of formation of the monomeric staple motif thus reduces to, how does $Au_4(SCH_3)_2$ form from a bare AuC interacting with thiols (Scheme 1)?

Scheme 1

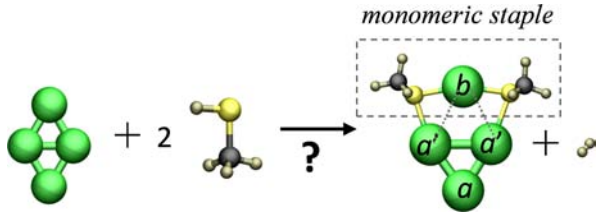

2.2. Simulation Details. AIMD simulations were performed within the Car−Parrinello approach,[22] which is based on DFT. The calculations were made using the generalized gradient-corrected approximation of the spin-dependent DFT (DFT-LSD), following the prescription of Perdew, Burke, and Ernzerhoff.[23] This functional has also been used in previous studies of AuCs (see, for instance, refs 17f and 19a), as well as in the study of the mechanism of CO_2 formation on a AuC.[24] The technical details of the calculations, as well as the initial tests on AuCs, are given in the Supporting Information. The starting configuration for the simulations consists of a naked Au_4 cluster with two/four methylthiol groups at ≈4 Å distance.

The metadynamics approach,[25] in its extended Lagrangian version,[26] was used to simulate the redox reaction. Metadynamics is a recently developed molecular dynamics technique aimed at enhancing the sampling of the phase space and at estimating the free-energy landscape (see pp S7 and S8 in the SI). This method has already been applied to a variety of topics in the fields of biophysics, chemistry, and materials science.[27]

The collective variables (CVs) used for the simulation of the redox reaction were taken as a combination of coordination numbers (CNs) of the covalent bonds being formed/broken. The CN is given by[26]

$$CN_{ij} = \frac{1 - \left(\frac{d_{ij}}{d^0}\right)^p}{1 - \left(\frac{d_{ij}}{d^0}\right)^{p+q}}$$

dx.doi.org/10.1021/ic301079k | Inorg. Chem. 2012, 51, 11422−11429

where d_{ij} is the internuclear distance of the atoms involved, d^0 is the threshold bonding distance, and p and q are exponents that determine the steepness of CN_{ij} decay with respect to d_{ij}. CN values range from 0 (not bonded) to 1 (bonded). These types of CVs have proven to be very useful for the description of chemical reactions in recent studies (see, for instance, refs 27c and 28).

Exploratory simulations including the CNs of all possible covalent bonds formed/broken (i.e., H−Au, H−H, S−H, and S−Au) revealed that the two hydrogen atoms are transferred sequentially (i.e., the second one "waits" for the first to be transferred). Therefore, we decided to model the redox reaction in two consecutive bidimensional metadynamics simulations (MTD1 and MTD2), corresponding to the respective transfers of H′ and H″. The first CV used for MTD1 (CV_1 or *H′ detachment*) measures the cleavage of the S−H′ bond and the formation of H−Au bonds, whereas the second one (CV_2 or *H′−Au coordination*) captures the diffusion of H′ on the AuC (see the SI). Concerning MTD2, the first collective variable (CV_1 or *H″ detachment*) measures the cleavage of the S−H″ bond and the formation of H_2, whereas the second one (CV_2 or *H−Au coordination*) captures the diffusion of both H′ and H″ on the AuC. Further details of the CVs used are described in the SI.

3. RESULTS AND DISCUSSION

3.1. Molecular Mechanism of the Redox Reaction. *Spontaneous Thiol Chemisorption.* We started our study by considering the smallest thioAuC bearing one staple motif, which is $Au_4(SCH_3)_2$ (see section 2.1). The first step of the formation of this thioAuC is the binding of two thiols to a Au_4 cluster. An AIMD simulation at room temperature shows that thiol binding occurs spontaneously in less than 2 ps, forming a Y-shaped thiol−gold complex (Figure 2). Chemisorption of the first thiol

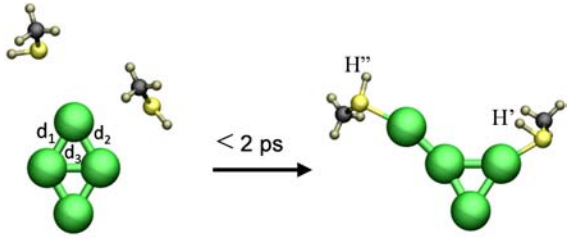

Figure 2. Spontaneous binding of thiols to the AuC (**R** → **I1**). The two thiols are initially located at a ≈4 Å distance from the cluster.

Table 1. Energetics of Chemisorption of One Thiol Group to thioAuC: $Au_4(CH_3SH)_{n-1} \xrightarrow{\Delta E} Au_4(CH_3SH)_n$

n	ΔE (kcal/mol)	n	ΔE (kcal/mol)
1	−8.7	3	−14.9
2	−19.3	4	>0

stabilizes the complex by 8.7 kcal/mol (Table 1), but the energy gain for binding the second thiol is more than twice that (19.3 kcal/mol), indicating that thiol chemisorption is initially cooperative. Interestingly, the AuC becomes slightly anionic (by 0.3 electrons; Table S3 in the SI) because of electron donation from the bound thiols. No further structural changes were observed when the simulation in time was extended. For this reason, we used an enhanced sampling technique (metadynamics) to activate the redox reaction and obtain its complete free-energy landscape.

Proton Transfer. The free-energy landscape reconstructed from the metadynamics simulations (Figure 3) contains a number of local minima (labeled **I1**−**I5**), expanding a narrow-energy window. Nevertheless, a reactive pathway connecting reactants and products can be easily drawn. The reaction begins with elongation of the S−H′ bond (by ∼0.2 Å; Table 2) until H′ starts to interact with the gold atoms (intermediates **I2** and **I3**). Similar configurations have been observed for a tryptophan amino acid absorbed on a AuC as very stable configurations, although the interaction takes place in this case via a carboxylic group instead of a thiol.[29] These intermediates, in which H′ is ready to be transferred to the cluster, can be described as "preactivated states". The reaction continues with the transfer of H′ into the Y-shaped cluster (**I2** to **I4**). At this point, H′ diffuses on the cluster, adopting various types of H−Au coordination (2- or 3-fold as in **I5**). From an energetic point of view, the transition from the reactants to a preactivated state (**I2** or **I3**) involves lower energetic barriers (16 kcal/mol) than proton transfer to the AuC (28 kcal/mol).

It is interesting to analyze the evolution of the atomic charges obtained from the electron density (solid lines in Figure 4 and Table S3 in the SI). The charge on H′ becomes slightly positive when H′ starts to interact with the cluster (**R** to **I1**). In turn, the sulfur atoms become more negative (Table S3 in the SI). However, the H′ charge decreases dramatically upon proton transfer (**I1** to **I4**; Figure 4). Remarkably, the charge of the AuC shows the opposite trend; it receives electron density upon thiol binding (**R** to **I1**) but becomes positively charged upon H′ transfer (from **I1** to **I4**). These changes indicate that H′ detaches from its thiol as a proton, but *it acquires pseudohydride character once bound to the cluster.*

Hydrogen Release. After the first proton (H′) is transferred, the second one (H″) starts to detach from the thiol and coordinates with the gold atoms. Simultaneously, one of the Au−Au bonds breaks (see the evolution of the main Au−Au distances in Table 2) and one gold atom separates from the rest (**I6**), forming the precursor of a staple motif. Finally, cleavage of the two Au−H bonds (**I7** to **P**) leads to the release of a hydrogen molecule and the formation of the staple motif. Therefore, the results demonstrate that *a monomeric staple motif can form in a redox reaction* (see the discussion in the SI, section 1) *from a AuC interacting with thiols.*

Excess of Bound Thiols Increasing Charge Transfer. Additional simulations were performed to study the mechanism in the presence of an excess of thiol groups. This scenario was modeled by considering two additional methylthiol molecules (Figure 5). In principle, only two thiols should lead to thiolate−sulfur bonds; otherwise, the resulting thioAuC would not conform to the electron count rules for exceptional stability (see the SI, p S2, eq 5).[19] However, any of the remaining two thiols could bind to the cluster as neutral thiols.

In fact, the initial AIMD simulation shows that three of the four thiols spontaneously bind to AuC (Figure 5) and the cluster remains closed at **I1**, unlike the previous case (Figure 3). All attempts to bind the fourth methylthiol were unsuccessful. Once it approaches the cluster, another methylthiol unbinds, recovering the initial configuration. This type of anticooperative effect is also reflected in the calculation of the binding energies (Table 1): thiol binding is initially favored by the binding of another one but later becomes less favored as the number of bound thiols increases. Therefore, there seems to be a maximum number of thiols that the cluster can accommodate. Interestingly, charge transfer from the thiol groups to AuC upon binding increases significantly with respect to the previous scenario with only two thiols (0.6 vs 0.3 electrons, respectively; compare the

dx.doi.org/10.1021/ic301079k | Inorg. Chem. 2012, 51, 11422−11429

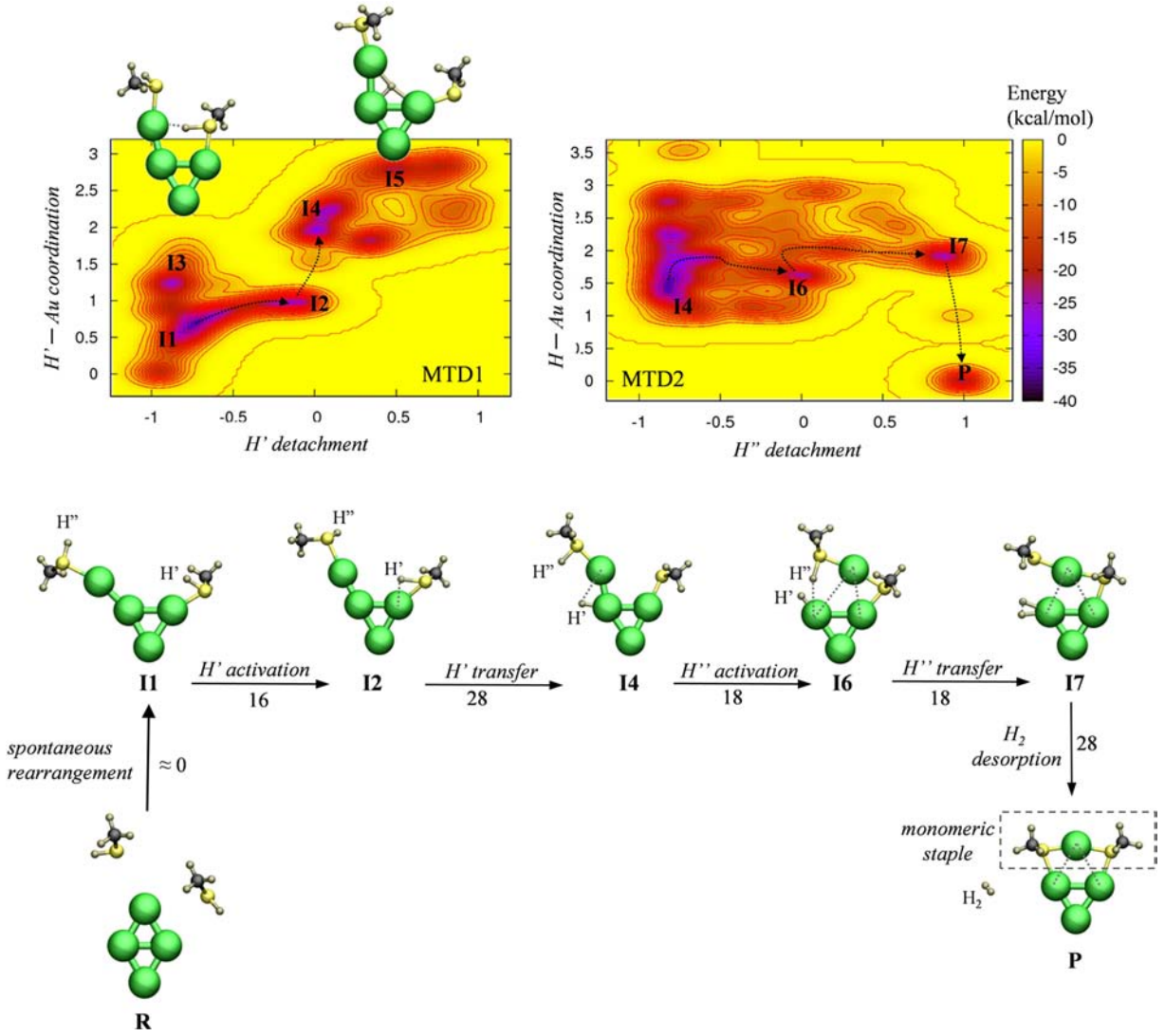

Figure 3. Free-energy surfaces reconstructed from the metadynamics simulations (MTD1 and MTD2) of the reaction of two CH_3SH molecules with Au_4. Contour lines are plotted every 2 kcal/mol. Au−Au solid bonds are drawn for distances of <2.8 Å, whereas a dashed line is used for bond distances in the range of 2.8−3.7 Å. Analogously, H−Au solid bonds are shown for distances of <1.85 Å, whereas dotted lines are used for bond distances in the range of 1.85−2.0 Å. Free-energy barriers (in kcal/mol) are shown below the arrows.

Table 2. Structural Parameters of Each Characteristic Point along the Reaction Pathway for the Reaction of Two Thiols with Au_4 (See Figure 3)

	distance (Å)							
	I1	**I2**	**I3**	**I4**	**I5**	**I6**	**I7**	**P**
Au−Au (d_1)	2.60 ± 0.06	2.53 ± 0.09	2.56 ± 0.04	2.61 ± 0.07	2.63 ± 0.05	3.70 ± 0.20	2.83 ± 0.02	2.90 ± 0.10
Au−Au (d_2)	4.50 ± 0.30	4.40 ± 0.10	4.11 ± 0.01	4.00 ± 0.01	3.93 ± 0.07	2.99 ± 0.05	3.10 ± 0.10	2.98 ± 0.08
Au−Au (d_3)	2.81 ± 0.09	2.65 ± 0.01	2.77 ± 0.02	2.68 ± 0.07	2.82 ± 0.05	2.94 ± 0.05	2.70 ± 0.10	2.94 ± 0.2
Au−S′	2.46 ± 0.07	2.4 ± 0.10	2.40 ± 0.06	2.29 ± 0.07	2.33 ± 0.06	2.36 ± 0.09	2.32 ± 0.04	2.39 ± 0.08
						2.37 ± 0.03	2.43 ± 0.04	2.41 ± 0.08
Au−S″	2.50 ± 0.10	2.46 ± 0.05	2.5 ± 0.10	2.41 ± 0.06	2.42 ± 0.09	2.38 ± 0.06	2.32 ± 0.04	2.60 ± 0.30
H′−S	1.39 ± 0.03[a]	1.56 ± 0.07	1.50 ± 0.05					
H″−S	1.38 ± 0.02	1.38 ± 0.02	1.38 ± 0.01	1.38 ± 0.01	1.38 ± 0.01	1.54 ± 0.09		
H′−Au		1.73 ± 0.04	2.0 ± 0.10	1.9 ± 0.10	2.01 ± 0.03	1.63 ± 0.07	1.8 ± 0.10	
				1.8 ± 0.10	1.95 ± 0.08			
					1.73 ± 0.06			
H″−Au						2.5 ± 0.1	1.85 ± 0.09	
H′−H″							0.85 ± 0.03	0.75 ± 0.01

[a]Standard deviation.

dx.doi.org/10.1021/ic301079k | Inorg. Chem. 2012, 51, 11422−11429

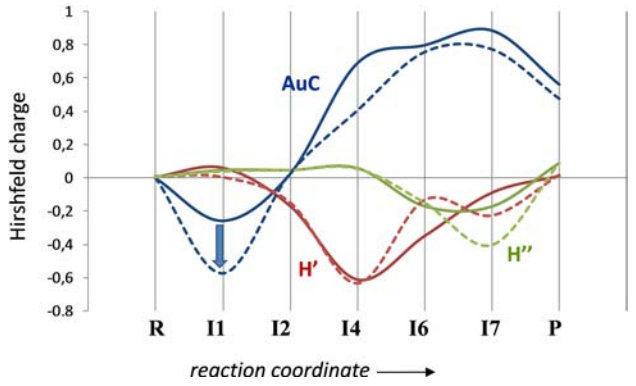

Figure 4. Evolution of atomic charges (Hirshfeld analysis) of AuC and the thiol hydrogen atoms along the reaction pathway. The charges are given relative to the isolated Au_4 and CH_3SH molecules. Solid line: reaction with two thiol molecules. Dashed line: reaction with four thiol molecules.

solid or dashed AuC lines in Figure 4). Clearly, *the AuC becomes more basic as more thiols bind to it, and this prevents opening of the cluster.*

Excess of Thiols Facilitating Proton Transfer. As in the previous simulations with two thiols, the computed free-energy surfaces (Figure 5) exhibit several local minima (**I1**–**I8**). A preactivated configuration in which H′ starts to interact with the cluster (**I2**) is also found (the S–H′ bond elongates by 0.12 Å with respect to the first intermediate; Table S5 in the SI). Remarkably, the transfer of the first thiol proton (**I2** → **I4**) implies a much lower activation energy compared with the simulation with two thiols (18 vs 28 kcal/mol). This finding can be explained in terms of the differences in the AuC electron density in both cases: *the greater the cluster electron density, the easier it is to receive a proton*. As was previously found, the detachment and subsequent transfer of H″ leads to the formation of molecular hydrogen (**I6** → **I7**).

Substantial atomic rearrangement occurs during the reactive process. Specifically, one gold atom separates from the rest (**I4** to **I6**; see the evolution of the main Au–Au distances in Table S5 in the SI) and one thiolate group changes position to interact with two gold atoms, thus forming the precursor of a monomeric staple (**I7**). Finally, the hydrogen molecule leaves the cluster, and the monomeric staple comes into view (**P**′). As in the previous case, hydrogen transfer and formation of molecular hydrogen are the steps with the highest activation energies, with H_2 formation being rate-limiting.

During the entire process, the third methylthiol molecule remains either unbound (**I6**) or weakly bound to AuC (the binding energy of the S···Au interaction at **P**′, 8 kcal/mol, is significantly lower than the 15 kcal/mol value at **I1**). An attempt to transfer the proton of the third thiol (H‴) to AuC failed, resulting in the complete detachment of the thiol and the formation of $Au_4(CH_3SH)_2$ (**P**). All of these observations suggest that, although a certain excess of thiol molecules participates in the formation of the staple motifs (thiol binding favors proton transfer from other thiols onto the cluster), they easily detach from the cluster.

3.2. General Discussion. Mechanistic Proposal. As mentioned above, a number of questions related to the formation of thioAuC and thioAuNP structures have emerged from recent studies, namely, how does the shape of the AuC change upon "thiol protection" and what is the fate of the thiol protons released during thiol binding (can they form molecular hydrogen as observed for thiol binding to gold surfaces? Are SH–Au and H–Au bonds formed?) Because of the difficulties in trapping short-lived species along the reaction pathway, answering these questions using experimental probes is a major challenge. In fact, both thiol–gold and thiolate–gold interactions have been detected by spectroscopic and X-ray techniques, respectively.[11a,16] Theoretical methods can be of major value in this area because they can offer the mechanistic insight needed to answer the above questions.

The picture emerging from the present ab initio study is as follows (see Figures 3 and 5). First, the thiols attach to AuC in an almost spontaneous process. In so doing, some gold atoms to which the thiols are attached may rearrange, decreasing the number of gold–gold interactions in which they participate. Second, transfer of protons from a fraction of the attached thiols occurs immediately, followed by migration through AuC. Third, one gold atom with an attached thiol unbinds from the other gold atoms while making an Au–S bond with a neighboring attached thiolate. In that way, it remains bonded to the cluster through this thiolate. This is the precursor of a staple motif. Fourth, the hydrogen atom of the thiol attached to this "peculiar" gold atom is transferred to the neighboring gold with a singly bound hydrogen. In this way, both the staple motif precursor and two hydrogen atoms coordinated to the same gold atom are formed. Fifth, formation of the new Au–S completes the staple, while H_2 desorbs from this gold atom.

All of these steps are expected to be easier (i.e., lower free energy barriers) for larger cluster sizes, where the number of gold atoms is higher and the system may be less tense. It should be noted that the two gold atoms anchoring the two SR groups of the monomeric staple are nearest neighbors in $Au_4(SCH_3)_2$ but next-nearest neighbors in larger clusters (Figure 1). In these cases, the number of possible configurations would most likely increase, leading to a much richer energy landscape with a large number of alternative pathways. However, the essential steps should be the same. It could also be argued that the solution phase would favor different oxidation states of the reacting species with respect to the ones obtained in gas-phase calculations. However, the fact that a neutral aprotic solvent is used in experiments[9] suggests that the solvent would not play a major role in the process of staple formation. Thus, the full mechanism can be summarized as follows:

$$Au_4 + 4CH_3SH \rightarrow Au_4(CH_3SH)_3 + CH_3SH$$

(thiol chemisorption)

$$Au_4(CH_3SH)_3 \rightarrow SCH_3{-}Au_4H{-}(CH_3SH)$$

(transfer of one thiol proton)

$$SCH_3{-}Au_4H{-}(CH_3SH)_2 \rightarrow (SCH_3)_2{-}Au_4H_2{-}CH_3SH$$

(transfer of a second thiol proton)

$$(SCH_3)_2{-}Au_4H_2{-}CH_3SH \rightarrow (SCH_3)_2{-}Au_4 {-}CH_3SH + H_2$$

(release of molecular hydrogen and monomeric staple formation)

dx.doi.org/10.1021/ic301079k | *Inorg. Chem.* 2012, 51, 11422–11429

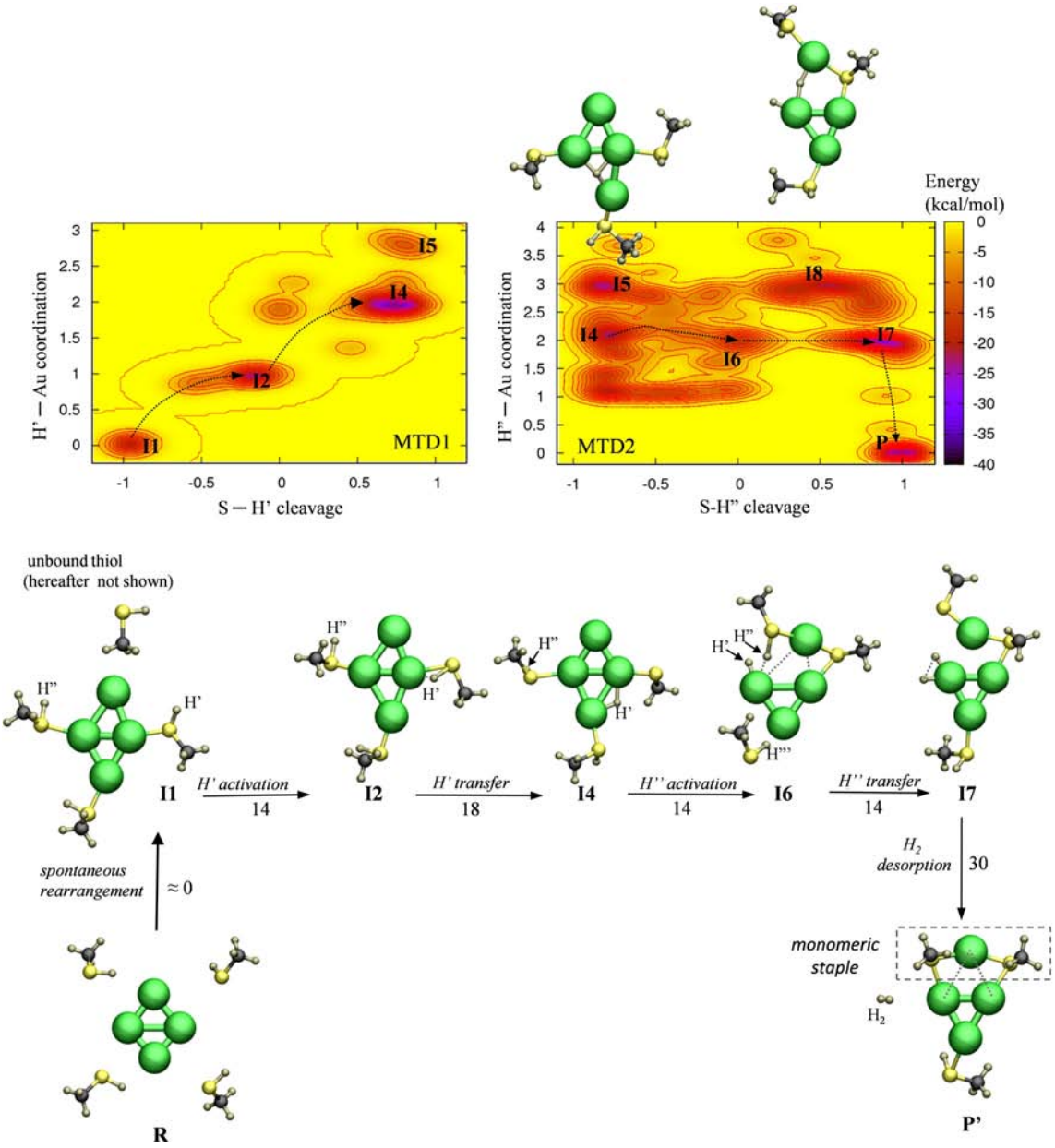

Figure 5. Free-energy surfaces reconstructed from the two metadynamics simulations of the reaction of four CH_3SH molecules with Au_4. Contour lines are plotted every 2 kcal/mol. Au—Au solid bonds are drawn for distances of <2.8 Å, whereas a dashed line is used for bond distances in the range of 2.8—3.7 Å. Analogously, H—Au solid bonds are shown for distances of <1.85 Å, whereas dotted lines are used for bond distances in the range of 1.85—2.0 Å. Free-energy barriers (in kcal/mol) are shown below the arrows.

$$(SCH_3)_2{-}Au_4{-}CH_3SH \rightarrow Au_4(SCH_3)_2 + CH_3SH$$

(excess thiol release)

An important conclusion that emerges from the calculations is that neutral bound thiols can be present either in the reaction intermediates or as part of the final product, in agreement with the interpretations of spectroscopic experiments from solutions of AuCs.[16] However, thiol binding is found to be weak, and therefore these extra thiols can easily detach from the cluster (Figure 5). Under this scenario, it is likely that the media surrounding the cluster determines the presence of neutral thiols in the final product. We believe this reconciles the fact that intact thiols on AuCs and AuNPs are detected in solution experiments but not in the crystalline phase.

Interestingly, thiol binding induces subtle but relevant electronic changes in AuC. In particular, the cluster receives charge from the thiol groups (Figure 4); i.e., it becomes more basic. The degree of charge transfer is more pronounced when there is an excess of bound thiols, thereby indicating that such an excess facilitates proton transfer. In fact, our results clearly show that in this situation the energy barrier for the first proton transfer drops off considerably; i.e., an excess of bound thiols favors the redox reaction. However, there is a maximum number of thiol groups that can bind to the cluster (three in our case); otherwise, the binding energy becomes positive. The balance between both factors will determine the number of bound thiols. The results in Figures 3 and 5 also suggest that the cluster tends to form staples in such a way that the appropriate "magic number" is reached (two in our case, meaning that, following the analysis provided in

dx.doi.org/10.1021/ic301079k | Inorg. Chem. 2012, 51, 11422—11429

the SI, two gold atoms will become of the a′ type). Consequently, for larger clusters, the degree to which the initial number of valence electrons of the cluster deviates from the "magic number" may also be an important parameter in controlling the number of staples formed.

4. CONCLUDING REMARKS

In conclusion, we find that one staple motif readily forms in a multiple-pathway chemical reaction when a AuC interacts with thiols, releasing molecular hydrogen. Both H−Au bonds and intact Au−thiol bonds are present during the reactive process, but the former are weakly bound and easily detach from the cluster. This explains why experimental detection of these species has been elusive and reconciles the interpretations of experimental studies in the crystalline and solution phases. Finally, we propose a mechanism in which an excess of bound thiols triggers the redox reaction by facilitating proton-transfer events. The results obtained in this study open the door for investigating the complex reaction pathways of peptide binding to AuNPs by ab initio metadynamics techniques. Investigations in this direction are currently underway in our laboratory.

■ ASSOCIATED CONTENT

Supporting Information

Further simulation details, structure/stoichiometric analysis, initial calculations on $Au_4(SCH_3)_2$, test of DFT parameters, and additional charge analysis. This material is available free of charge via the Internet at http://pubs.acs.org.

■ AUTHOR INFORMATION

Corresponding Author

*E-mail: crovira@pcb.ub.es.

Notes

The authors declare no competing financial interest.

■ ACKNOWLEDGMENTS

We acknowledge the Spanish Ministry of Economy and Competitiveness (MINECO; Grants CTQ2011-25871 and BIO2008-00799) and the Generalitat de Catalunya (GENCAT; Grants 2009SGR-1309, 2009SGR-1005, and XRB) for their financial assistance. V.R.-C. acknowledges a FPU fellowship from MINECO. We acknowledge the computer support, technical expertise, and assistance provided by the Barcelona Supercomputing Center−Centro Nacional de Supercomputación (BSC−CNS).

■ REFERENCES

(1) (a) Schmid, G. *Chem. Soc. Rev.* **2008**, *37*, 1909−1930. (b) Schmid, G.; Corain, B. *Eur. J. Inorg. Chem.* . **2003**, 3081−3098.

(2) (a) Reichert, J.; Ochs, R.; Beckmann, D.; Weber, H. B.; Mayor, M.; Lohneysen, H. V. *Phys. Rev. Lett.* **2002**, *88*, 176804. (b) Zhou, C.; Deshpande, M. R.; Reed, M. A.; Jones, L.; Tour, J. M. *Appl. Phys. Lett.* **1997**, *71*, 611−613.

(3) (a) Metallo, S. J.; Kane, R. S.; Holmlin, R. E.; Whitesides, G. M. *J. Am. Chem. Soc.* **2003**, *125*, 4534−4540. (b) Dubois, L. H.; Nuzzo, R. G. *Annu. Rev. Phys. Chem.* **1992**, *43*, 437−463. (c) Ulman, A. *Chem. Rev.* **1996**, *96*, 1533−1554.

(4) Shaw, C. F. *Chem. Rev.* **1999**, *99*, 2589−2600.

(5) (a) Penn, S. G.; He, L.; Natan, M. J. *Curr. Opin. Chem. Biol.* **2003**, *7*, 609−615. (b) Guerrero, S.; Araya, E.; Fiedler, J. L.; Arias, J. I.; Adura, C.; Albericio, F.; Giralt, E.; Arias, J. L.; Fernandez, M. S.; Kogan, M. J. *Nanomedicine (London)* **2010**, *5*, 897−913. (c) Parveen, S.; Misra, R.; Sahoo, S. K. *Nanomedicine* **2012**, *8*, 147−166.

(6) Kogan, M. J.; Bastus, N. G.; Amigo, R.; Grillo-Bosch, D.; Araya, E.; Turiel, A.; Labarta, A.; Giralt, E.; Puntes, V. F. *Nano Lett.* **2006**, *6*, 110−115.

(7) Duncan, B.; Kim, C.; Rotello, V. M. *J. Controlled Release* **2010**, *148*, 122−127.

(8) Li, G. T.; Lauer, M.; Schulz, A.; Boettcher, C.; Li, F. T.; Fuhrhop, J. H. *Langmuir* **2003**, *19*, 6483−6491.

(9) Matthiesen, J. E.; Jose, D.; Sorensen, C. M.; Klabunde, K. J. *J. Am. Chem. Soc.* **2012**, *134*, 9376−9379.

(10) Letardi, S.; Cleri, F. *J. Chem. Phys.* **2004**, *120*, 10062−10068.

(11) (a) Jadzinsky, P. D.; Calero, G.; Ackerson, C. J.; Bushnell, D. A.; Kornberg, R. D. *Science* **2007**, *318*, 430−433. (b) Qian, H.; Eckenhoff, W. T.; Zhu, Y.; Pintauer, T.; Jin, R. *J. Am. Chem. Soc.* **2010**, *132*, 8280−8281. (c) Heaven, M. W.; Dass, A.; White, P. S.; Holt, K. M.; Murray, R. W. *J. Am. Chem. Soc.* **2008**, *130*, 3754−3755.

(12) (a) Maksymovych, P.; Sorescu, D. C.; Yates, J. T., Jr. *Phys. Rev. Lett.* **2006**, *97*, 146103. (b) Mazzarello, R.; Cossaro, A.; Verdini, A.; Rousseau, R.; Casalis, L.; Danisman, M. F.; Floreano, L.; Scandolo, S.; Morgante, A.; Scoles, G. *Phys. Rev. Lett.* **2007**, *98*, 016102. (c) Maksymovych, P.; Voznyy, O.; Dougherty, D. B.; Sorescu, D. C.; Yates, J. T., Jr. *Prog. Surf. Sci.* **2010**, *85*, 206−240.

(13) Jiang, D. E.; Tiago, M. L.; Luo, W.; Dai, S. *J. Am. Chem. Soc.* **2008**, *130*, 2777−2779.

(14) Hakkinen, H.; Walter, M.; Gronbeck, H. *J. Phys. Chem. B* **2006**, *110*, 9927−9931.

(15) (a) Pei, Y.; Gao, Y.; Zeng, X. C. *J. Am. Chem. Soc.* **2008**, *130*, 7830−7832. (b) Akola, J.; Walter, M.; Whetten, R. L.; Hakkinen, H.; Gronbeck, H. *J. Am. Chem. Soc.* **2008**, *130*, 3756−3757.

(16) Hasan, M.; Bethell, D.; Brust, M. *J. Am. Chem. Soc.* **2002**, *124*, 1132−1133.

(17) (a) Konopka, M.; Rousseau, R.; Stich, I.; Marx, D. *J. Am. Chem. Soc.* **2004**, *126*, 12103−12111. (b) Kruger, D.; Fuchs, H.; Rousseau, R.; Marx, D.; Parrinello, M. *J. Chem. Phys.* **2001**, *115*, 4776−4786. (c) Santarossa, G.; Vargas, A.; Iannuzzi, M.; Baiker, A. *Phys. Rev. B* **2010**, *81*, 174205. (d) Gronbeck, H.; Curioni, A.; Andreoni, W. *J. Am. Chem. Soc.* **2000**, *122*, 3839−3842. (e) Garzon, I. L.; Rovira, C.; Michaelian, K.; Beltran, M. R.; Ordejon, P.; Junquera, J.; Sanchez-Portal, D.; Artacho, E.; Soler, J. M. *Phys. Rev. Lett.* **2000**, *85*, 5250−5251. (f) Tlahuice, A.; Garzon, I. L. *Phys. Chem. Chem. Phys.* **2012**, *14*, 7321−7329.

(18) Askerka, M.; Pichugina, D.; Kuz'menko, N.; Shestakov, A. *J. Phys. Chem. A* **2012**, *116*, 7686−7693.

(19) (a) Walter, M.; Akola, J.; Lopez-Acevedo, O.; Jadzinsky, P. D.; Calero, G.; Ackerson, C. J.; Whetten, R. L.; Gronbeck, H.; Hakkinen, H. *Proc. Natl. Acad. Sci. U.S.A.* **2008**, *105*, 9157−9162. (b) Knight, W. D.; Clemenger, K.; Deheer, W. A.; Saunders, W. A.; Chou, M. Y.; Cohen, M. L. *Phys. Rev. Lett.* **1984**, *52*, 2141−2143. (c) Deheer, W. A. *Rev. Mod. Phys.* **1993**, *65*, 611−676.

(20) (a) Jiang, D. E.; Whetten, R. L.; Luo, W. D.; Dai, S. *J. Phys. Chem. C* **2009**, *113*, 17291−17295. (b) Jiang, D. E.; Chen, W.; Whetten, R. L.; Chen, Z. F. *J. Phys. Chem. C* **2009**, *113*, 16983−16987.

(21) Bonasia, P. J.; Gindelberger, D. E.; Arnold, J. *Inorg. Chem.* **1993**, *32*, 5126−5131.

(22) Car, R.; Parrinello, M. *Phys. Rev. Lett.* **1985**, *55*, 2471−2474.

(23) Perdew, J. P.; Burke, K.; Ernzerhof, M. *Phys. Rev. Lett.* **1996**, *77*, 3865−3868.

(24) Lopez-Acevedo, O.; Kacprzak, K. A.; Akola, J.; Hakkinen, H. *Nat. Chem.* **2010**, *2*, 329−334.

(25) Laio, A.; Parrinello, M. *Proc. Natl. Acad. Sci. U.S.A.* **2002**, *99*, 12562−12566.

(26) Iannuzzi, M.; Laio, A.; Parrinello, M. *Phys. Rev. Lett.* **2003**, *90*, 238302.

(27) (a) Sun, J.; Klug, D. D.; Martonak, R.; Montoya, J. A.; Lee, M. S.; Scandolo, S.; Tosatti, E. *Proc. Natl. Acad. Sci. U.S.A.* **2009**, *106*, 6077−6081. (b) Biarnes, X.; Ardevol, A.; Planas, A.; Rovira, C.; Laio, A.; Parrinello, M. *J. Am. Chem. Soc.* **2007**, *129*, 10686−10693. (c) Ardevol, A.; Rovira, C. *Angew. Chem., Int. Ed.* **2011**, *50*, 10897−10901.

(28) (a) Comas-Vives, A.; Stirling, A.; Lledos, A.; Ujaque, G. *Chem.—Eur. J.* **2010**, *16*, 8738−8747. (b) Stirling, A.; Papai, I. *J. Phys. Chem. B*

2010, *114*, 16854−16859. (c) Alfonso-Prieto, M.; Biarnes, X.; Vidossich, P.; Rovira, C. *J. Am. Chem. Soc.* **2009**, *131*, 11751−11761. (d) Biarnes, X.; Ardevol, A.; Iglesias-Fernandez, J.; Planas, A.; Rovira, C. *J. Am. Chem. Soc.* **2011**, *133*, 20301−20309. (e) Nair, N. N.; Schreiner, E.; Marx, D. *J. Am. Chem. Soc.* **2008**, *130*, 14148−14160.

(29) Joshi, P.; Shewale, V.; Pandey, R. *J. Phys. Chem. C* **2011**, *115*, 22818−22826.